Silicates and Aromatic Hydrocarbons in the 10 μm Spectrum of the Taurus Dark Cloud Source. Elias 1.

Martha S. Hanner and Timothy Y. Brooke[a]
Mail Stop 183-601
Jet Propulsion Laboratory
California Institute of Technology
4800 Oak Grove Drive
Pasadena, CA 91109

and

Alan 'T'. Tokunaga
Institute for Astronomy
University of Hawaii
2680 Woodlawn Drive
Honolulu, HI 96822

To be submitted to ***Astrophysical*** *Journal Letters*

May 1994

[a]NAS/NRC Resident Research **Associate.**

ABSTRACT

We have obtained 10.4-12 μm spectra at spectral resolution R ≈ 190 of the Herbig Ae star Elias 1 in the Taurus dark cloud with the UKIRT CGS3 spectrometer, along with an 8-13 μm spectrum at R ≈ 55. The 11.2 μm emission feature matches the wavelength, shape, and FWHM of the 11.22 μm aromatic hydrocarbon band, consistent with the presence of other aromatic features. A strong 11.06 μm feature is present and new emission features at 11.6 and 11.76 μm are revealed. The strong silicate emission feature is broader and peaks at a longer wavelength than can be reproduced with the Trapezium emissivity. Larger grains, with mean radius a ≥ 1.5 μm appear to be required, a possible indication of grain growth around a young star.

1. INTRODUCTION

The pre-main-sequence object Hiss 1 is a Herbig Ac star in the Taurus dark cloud with an unusual infrared spectrum. Both strong silicate emission and the family of aromatic hydrocarbon bands arc present, as WC]] as the anomalous 3.43 and 3.53 μm features (Whittet *et al.* 1983; Tokunaga *et al.* 1991; Schutte *et al.* 1990). The silicate feature is unlike that seen in other young stellar objects in the Taurus region (Cohen and Witteborn 198S; Whittet *et al.* 1988) or in the *p* Oph cloud (Hanner, Brooke, and Tokunaga 1994; hereafter Paper 1). Schutte *et al.* have suggested that the emission peak at 11.2 μm could be *due.* to crystalline olivine, similar to that seen in comet Halley. If true, this result would be significant in linking the silicate grains in comets, which rcpre.sent the proto-solar nebula, with those in proto-stellar dust clouds.

in order to study the silicate and organic dust around Elias 1, wc obtained a new low resolution 10 μm spectrum and a higher resolution spectrum near 11 pm. These data show that the 11.2 μm feature is primarily the normal 11.22 μm aromatic hydrocarbon feature, with a strong 11.06 μm feature. The ncw spectra allow us to remove the estimated contribution from the aromatic hydrocarbons and define better the emissivity of the silicate grains around Elias 1. The unusually broad silicate feature may reflect grain growth around this young star.

2. OBSERVATIONS

The spectra of Elias 1 were acquired with the CGS3 10-20 μm grating spectrometer at the United Kingdom Infrared Telescope (UKIRT) on 1993 Nov 4 and 6 (I-H'). The low-resolution 10 μm grating with R-55 and the high resolution grating with R-190 were employed with a 3.4" aperture and 20" EW chopping throw. Both nights were exceptionally dry and stable. Wavelength calibration was clone via a krypton lamp observed through a K filter at fourth, fifth, and sixth orders. The calibration was checked by measuring the emission lines in the planetary nebula NGC *702'7.* We estimate the wavelength uncertainty to be ±0.02 μm.

The low-resolution spectrum was taken on Nov 4, using two grating positions spaced approximately one-half resolution element apart (Fig. 1), The standard star was α Tau. Alpha Tau was calibrated versus Sirius, which was assumed to have a color temperature of 10,000 K and a flux 4.33 x 10^{-12} W/m^2/μm at 10.1 μm. I ligh-resolution spectra covering, λ 10.4 to 12.0 μm were obtained on Nov 4 and Nov 6, using three grating positions to give 3 points pcr resolution element (Fig. 2). The standard star was α Tau; wc assumed that its spectrum was smooth al this resolution.

3. THE AROMATIC 1 IYDROCARBON EMISSION BANDS

Features at 8.6 pm, 11.2 pm, and a rise at $\lambda < 8$ μm are visible in the low resolution spectrum (Fig. 1), corresponding to the well-known series of emission bands at 7.7, 8.65, and 11.22 pm. These are generally attributed to vibrations in polycyclic aromatic hydrocarbons (PAI 1s), existing either as free molecules, PAH clusters, or within larger hydrogenated amorphous carbon particles (Duley & Williams 1981; Leger & Puget 1984; Allamandola, Tielens & Barker 1985) or to aromatic hydrocarbon components in an amorphous material (Sakata *et al.* 1987). The 11.2 μm feature. is resolved and new spectral structure is revealed in the higher resolu tion spect ra present cd in Fig. 2,

To analyze the shape of the 11.2 μm peak, we subtracted a linear continuum fit at 10.95 μm and 11.50 μm and averaged the Nov 4 and Nov 6 spectra (Fig. 3). The main feature matches the peak position (1 1.22 pm), asymmetric shape, and FWI IM (0.22 μm) of the aromatic hydrocarbon band in other sources (Witteborn *et* al. 1989). The integrated flux is $17.5 \pm 0.4 \times 10^{-15}$ W/m^2. The narrow peak at 11.31 μm is possibly the 9-7 transition in atomic hydrogen (211.309 μmin vacuum; Moore 1949). If so, the adjacent points are the half-power points and also lie above the emission band profile. (For comparison, the 8.6 μm feature in Fig. 1 has central wavelength 8.65 pm, FWI IM 0.21 pm, and integrated flux $16.7 \pm 0.6 \times 10^{-15}$ W/m^2.)

Schutte *et al.* (1990) suggested that the spectral peak near 11.2 μm in Elias 1 could be due to crystalline olivine, similar to that in Comet Halley. While some contribution from silicate emission cannot be ruled out, we conclude that crystalline olivine is not the major source of the 11.22 μm feature in Elias 1.

The secondary maximum at 11.06 μm has an integrated flux of $4 \pm 0.2 \times 10^{-15}$ W/m^2. This is stronger relative to the 11.22 μm feature than any of the sources observed by Witteborn *et al.* (1989) or Roche, Aitken, and Smith (1991), with the exception of the pre-main-sequence object TY G-A. A strong 11.06 μm feature does not correlate with the anomalous 3.43 and 3.53 μm emission bands, since these bands are absent in TY CrA (T. Geballe, private communication). HD 97048, which also exhibits the 3.43 and 3.53 μm bands has only a weak 11.06 μm feature.

We have identified two new features in Miss 1 at λ 11.6 μm and 11.76 μm (Fig. 2). These new features satisfy the criteria that they are several data points wide and are present in both the Nov. 4 and Nov. 6 spectra. Their integrated fluxes are about 10% that of the 11.22 μm feature. Possible spectral structure is present in the 10.4 -10.8 μm region, but higher signal/noise data are required to confirm this. in ratios of our high-resolution spectra of α Tau separated by 0.32 in air mass, only one possible atmospheric feature greater than 1 percent is evident, near 11.73 μm. The difference in air mass between Elias 1 and α Tau was 0.15 on Nov 4 and only 0.01 on Nov 6. 'Thus, we believe that none of the features in Fig. 2 are atmospheric in origin.

The 11.22 μm and 11.06 μm features are believed to be due to cmt-of-plane bending mode vibrations within aromatic rings containing only nonadjacent peripheral hydrogen atoms (Allamandola *et al.* 1989; Leger *et al.* 1989). The frequency of the C-H bending mode depends on the number of adjacent hydrogen atoms in the. peripheral rings of PAH molecules; the frequency decreases as the number of peripheral H atoms increases. In this interpretation, the band at 11.6 μm could arise from one or two peripheral H atoms, while the 11.'76 μm band suggests two peripheral H atoms.

4. THE SILICATE EMISSION FEATURE

4.1 *Removing the aromatic hydrocarbon features*

in order to define the silicate emissivity from the low resolution spectrum, it is necessary to remove the contribution of the aromatic hydrocarbon emission features. Fluxes in the 11.2 and 11.06 μm features were estimated from the high resolution data of 4 Nov assuming a linear baseline between 10.95 and 11.50 μm. The points were then convolved to the. spectral resolution of the low resolution data and subtracted. The contribution of the aromatic 7.7 μm feature is more difficult to estimate. Only part of the. feature is accessible from the ground. A spectrum of Elias 1 from 5-8 μm taken from the Kuiper Airborne Observatory (Schutte *et al.* 1990) is shown with our spectrum in Fig. 4. The KAO spectrum was multiplied by a factor 1.15 to match the CGS3 spectrum in the region of

overlap (7.8-8.2 μm), but only the CGS3 points arc plotted in this range because of the much 10WCJ signal-to-noise of the KAO data.

We estimated the contribution of the 7.7 μm feature by assuming that the feature had approximately the same shape as the 7.7 μm feature in the Orion bar, position 4 (Fig. lb, Bregman *et al.* 1989). The Orion bar spectrum is useful for estimating the contribution of aromatics since the aromatic features dominate the, total flux. A precise spectral match was impossible since the Elias 1 spectrum rises much more sharply at $\lambda < 8$ μm than the Orion bar. Instead, wc fixed the relative fluxes at three points away from the peak (7.0,8.9, and 9.S μm) and the total integrated flux in the feature (normalized by the 7.() μm flux) at values taken from the. Orion bar spectrum, then determined the simplest continuum consistent with those valu es. The 8.6 μm region was not included. The result, a second order polynomial, is shown in Fig. 4. Replacing the points shortward of 9.5 μm by this continuum gives the spectrum shown by the dashed curve in Fig. 4. Note that - 30% of the total flux at 8.0 μm is due to the 7.7 μm feature.

Using a cubic spline fit to points where the 7.7 μm feature flux is assumed to be negligible (e.g. Cohen *et al.* 1986) did not change the resulting continuum in the 8 μm region by more than 596. We prefer the continuum derived above because it allows for the presence of "plateau" emission from carbonaceous grains at 7.0 μm (Bregman *et al.* 1989).

4.2 *Modeling the* ***silicate*** *feature*

The silicates along the lines of sight 10 many young stars in molecular clouds appear to have emissivities similar to that of the Trapezium region (Cohen and Witteborn 1985; Whittet *et al.* 1988; Paper 1). It is clear that the silicate emission feature in Elias 1 is not due solely to optically thin emission from grains with the Trapezium emissivity because the contrast is lower and the feature is broader than the Trapezium emissivity (see Fig. 1 in Paper 1). '1'here could be four explanations for this: 1) optical depth increase; 2) dilution of optically thin emission by featureless emission; 3) grain size increase; or 4) compositional difference in the silicates.

We tested whether (1) or (2) might explain the feature in Elias 1 using the Trapezium emissivity as a template in two simple models, described in Paper 1. Source functions in each case were assumed to be power laws. The parameters (optical depths, power laws, scale factors) were adjusted until the best]cast-squares fit to the data was obtained.

Case 1 - Variable optical depth

$$\lambda F_\lambda = a_0\left(\frac{\lambda}{9.7}\right)^m \left(1 - e^{-a_1 \epsilon_t(\lambda)}\right) \quad (1)$$

With $\epsilon_t(\lambda)$ normalized at 9.7 μm, the parameter a_1 is the total silicate optical depth at 9.7 μm, $\tau_{9.7}$. This slab model approximates a dusty envelope which both emits and absorbs at 10 pm.

Case 2 - *Two* component: Optically thick + optically thin emission

$$\lambda F_\lambda = a_0\left(\frac{\lambda}{9.7}\right)^n + a_2\left(\frac{\lambda}{9.7}\right)^m \epsilon_t(\lambda) \quad (2)$$

This model might apply, for example, to an optically thin envelope and an optically thick disk (or the star itself), both of which both contribute to the flux at 10 μm. The optically thick component could alternatively rcprc.sent emission from featureless dust.

Fig. 5a shows the best fit under case 1, with $\tau_{9.7} = 1.85$. The fit is poor; the Elias 1 spectrum clearly peaks at a longer wavelength, Case 2 provided a marginally better fit, but required steep power laws which do not match the published photometry of Hiss 1.

An increase in the grain size causes a broadening of the silicate emissivity toward longer wavelengths (Simpson 1991; 1 Ianner *et al.* 1994a). '1'0 test whether larger grains might provide a better fit to the Elias 1 spectrum, wc calculated absorption efficiencies, Q_{abs}, for spheres of different radii using the optical constants of astronomical silicate (Draine and 1 ,ee 1984). The best fit to the Elias 1 spectrum for case 1 was for a grain radius of 1.5 μm (Fig. 5b) with $\tau_{9.7} = 0.33$. A radius of 2.0 μm gave a significantly worse fit.

The model with a= 1.5 μm is significantly better than the fit with the Trapezium emissivity, suggesting that the mean size of the circumstellar grains near Elias 1 may be considerably larger than interstellar grains. But the Elias 1 spectrum peaks at a longer wavelength (-10.6 pm), so there may be a compositional diffcrcncc between the silicates around Elias 1 and the Trapezium region also. If such compositional differences broaden the silicate emissivity compared to the Trapezium, then larger grain size would not n ecessarily be rcqu ired. Grain growth is expected in protoplanetary disks. The silicate emission feature in β Pic was fit by Aitken *et al.* (1994) using astronomical silicate optical constants and grain sizes similar to those found here.

The silicate feature in 1 Elias 1 differs from that seen in comet Halley and some other comets (1 Ianner et al 1994a). The comet feature has a broad maximum near 9.8 μm (vs. -10.6 μm in Elias 1), an obvious dip at 10.7 μm, and a rise from 10.7 to the peak at 11.2 μm. "J'bus, wc conclude that the mineralogy of the silicates in Elias 1 is not the. same as cometary dust.

5. CONCLUSIONS

The 10.4 - 12 μm spectrum of Elias 1 in the Taurus dark cloud at spectral resolution R≈ 190 reveals considerable spectral detail. The profile of the emission feature at 11.22 μm matches the peak wavelength, asymmetric shape., and FWHM of the well-known aromatic hydrocarbon band. A prominent 11.06 μm feature is present. Two new features are detected at λ11.6 and 11.76 μm, with integrated fluxes - 10% that of the 11,22 μm feature.

A low resolution 8-13 μm spectrum was used to estimate the silicate emissivity after removal of the cent ribu t ion from the aromatic h ydrocarbons. The silicate feature is not well-matched by simple models incorporating the Trapezium emissivity, believed to be typical of molecular cloud dust. But the featu re is approximately reproduced by optically thin emission from the. "astronomical silicates" defined by Draine & Lee (1984) for grains with a mean radius - 1.5 pm. This may indicate that significant grain growth has begun in the circumstellar environment of this you ng stellar object. Alternatively, significant compositional differences may exist between 1 Hiss 1 and the Trapezium. The silicate feature does not resemble that of Comet Halley or other comets; thus, the silicate m ineralogy differs from cometary dust,

ACKNOWLEDGEMENTS

We thank the staff of the UKIRT for their support. UKIRT is operated by the Royal Observatory Edinburgh on behalf of the U.K. Science and Engineering Research Council. Part of this research was carried out at the Jet Propulsion laboratory, California Institute of Technology under contract with NASA. A.T. acknowledges the support of NASA grant NAGW-2278.

REFERENCES

Aitken, D. K., Moore, T. J. T., Roche, 1'. F., Smith, C. 11. and Wright, C. M. 1993, MNRAS 265, 141.

Allamandola, L. J., Tielens, A. G. G. M., and Barker, J. R. 1985, ApJ, 290, L25.

Allamondola, L. J., Tielens, A, G.G.M. and Barker, J. R. 19S9, ApJ Suppl., 71, 733.

Bregman, J. D., Allamandola, I.. J., Tielens, A. G. G. M., Geballe, T. R., and Witteborn, F. C. 1989, ApJ, 344, 798.

Cohen, M., and Witteborn, F. C. 1985, ApJ, 294, 345.

Draine, B. 'I'., and lee, H. M., 1984, ApJ, 285, 89.

Duley, W. W. and Williams, D. A. 1981, MNRAS, 196, 269.

Hanner, M. S., Brooke, T. Y., and Tokunaga, A. '1'. 1994b, ApJ, submitted.

1 Ianner, M. S., Lynch, D. K., and Russell, R. W. 1994a, ApJ, 42S, 274.

Leger, A., d'Hendecourt, 1.., and Defourneau, D. 1989, A&A, 216, 148.

Leger, A. and Puget, J. 1,.1984, A&A, 137, 1,6.

Moore, C. E. J949, Atomic Energy I evels, Vol. 1, NBS Circ. 467, Washington D.C.

Roche, P. F., Aitken, D. K., and Smith, C. }1. 1991, MNRAS, 2S2, 282.

Sakata, A., Wada, S. Onaka, T. and Tokunaga, A. T. 1987, ApJ, 320, 1.63.

Schutte, W. A., Tielens, A. G. G. M., Allamandola, L. J., Cohen, M. and Wooden, D. 11.1990, ApJ 360, 577.

Simpson, J. P. 1991, ApJ, 368, 570.

Tokunaga, A. T. Sellgren, K., Smith, R. G., Nagata, 'T'., Sakata, A., and Nakada, Y. 1991, ApJ , 380, 452.

Whittet, D. C.B., Bode, M. F., Longmore, A. J., Adamson, A. J., Mcliaclz.can, A. D., Aitken, D. K., and Roche, P. F. 1988, MNRAS, 233, 321.

Whittet, D.C.B., Williams, P. M., Bode, M. F., Davies, J. K., and Zealey, W. J. 1983, A&A, 123, 301.

Witteborn, F. C., Sandford, S. A., Bregman, J. D., Allamandola, L. J., Cohen, M., Wooden, 11. 11., and Graps, A. 1,.1989, ApJ, 341, 270.

FIGURE LEGENDS

Figure 1. Elias 1 CGS3 spectrum at spectral resolution R ≈ 55, Nov. 4, 1993.

Figure 2. Elias 1 CGS3 spectra at resolution R ≈ 190. Nov. 4 spectrum displaced by -1×10^{-13} and Nov. 6 spectrum displaced by $+1 \times 10^{-13}$ W/m^2/μm.

Figure 3. The 11,22 μm and 11.06 μm features in Elias 1. A linear continuum fit at A10.9S and 11.50 μm has been subtracted from the observed fluxes in Fig. 2 and the spectra from Nov. 4 and Nov. 6 have been averaged.

Figure 4. S-13 μm spectrum of Elias 1. Filled circles: CGS3 data from Fig. 1; open circles: KAO data from Schutte *et al.* (1990), multiplied by factor 1, 1S; Dashed line is the flux after removal of the aromatic hydrocarbon contribution (see text).

Figure 5a. Best fit Trapezium emissivity model (solid line) compared to Elias 1 silicate emission (points) for case 1, $\tau_{9.7} = 1.85$, $m = 1.61$.

Figure 5b. Best fit with "astronomical silicate" grains of radius a = 1.5 μm (solid line) and a = 2.0 μm (dashed line) for case 1, $\tau_{9.7} = 0.34$, $m = -1.13$.

Figure 1

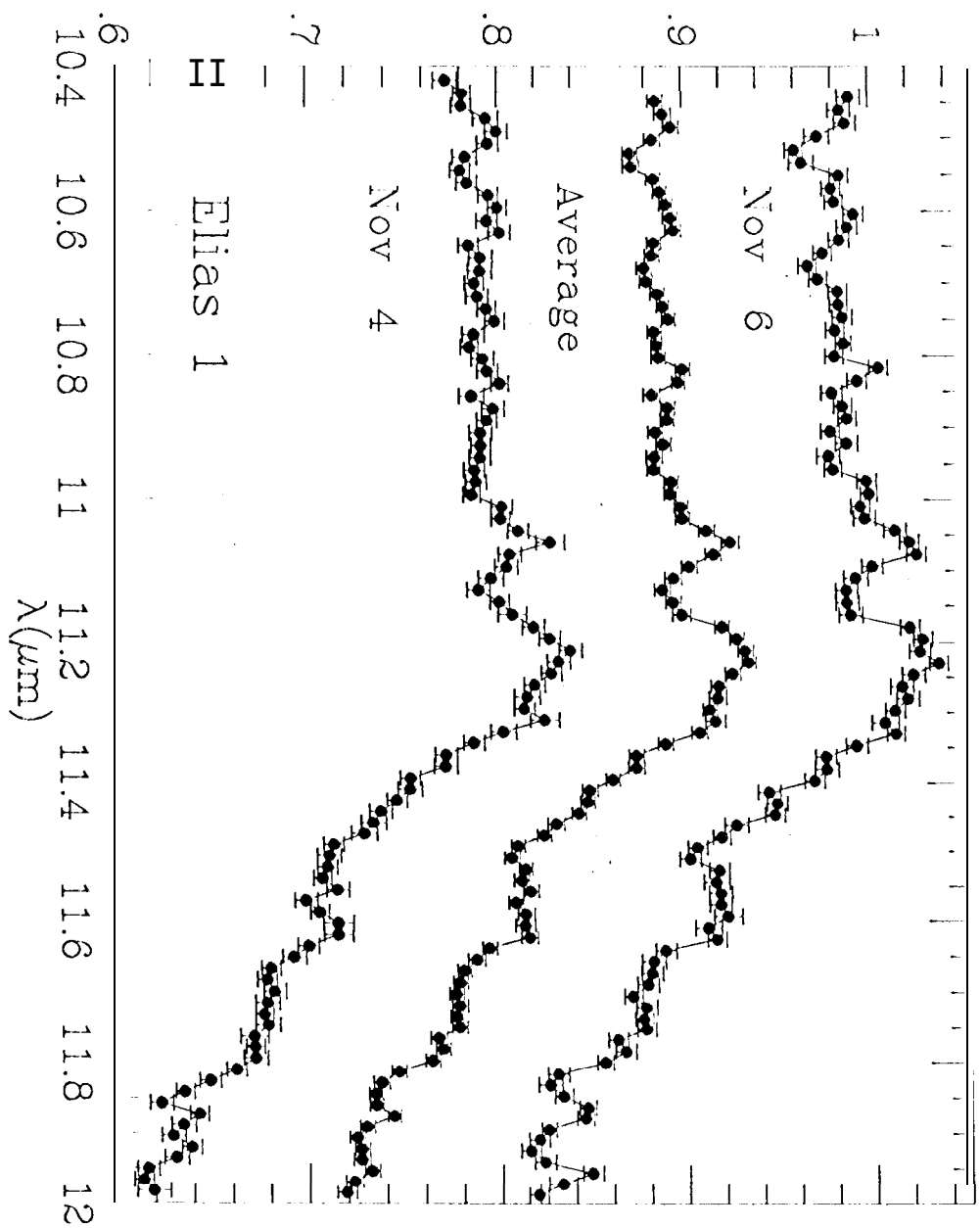
Flux 1 ()12 (W/m^2/μm)
.6
.7
.8
.9
1
10.4
10.6
10.8
11
11.2
11.4
11.6
11.8
12
λ(μm)
II
Elias 1
Nov 4
Average
Nov 6

Figure 2

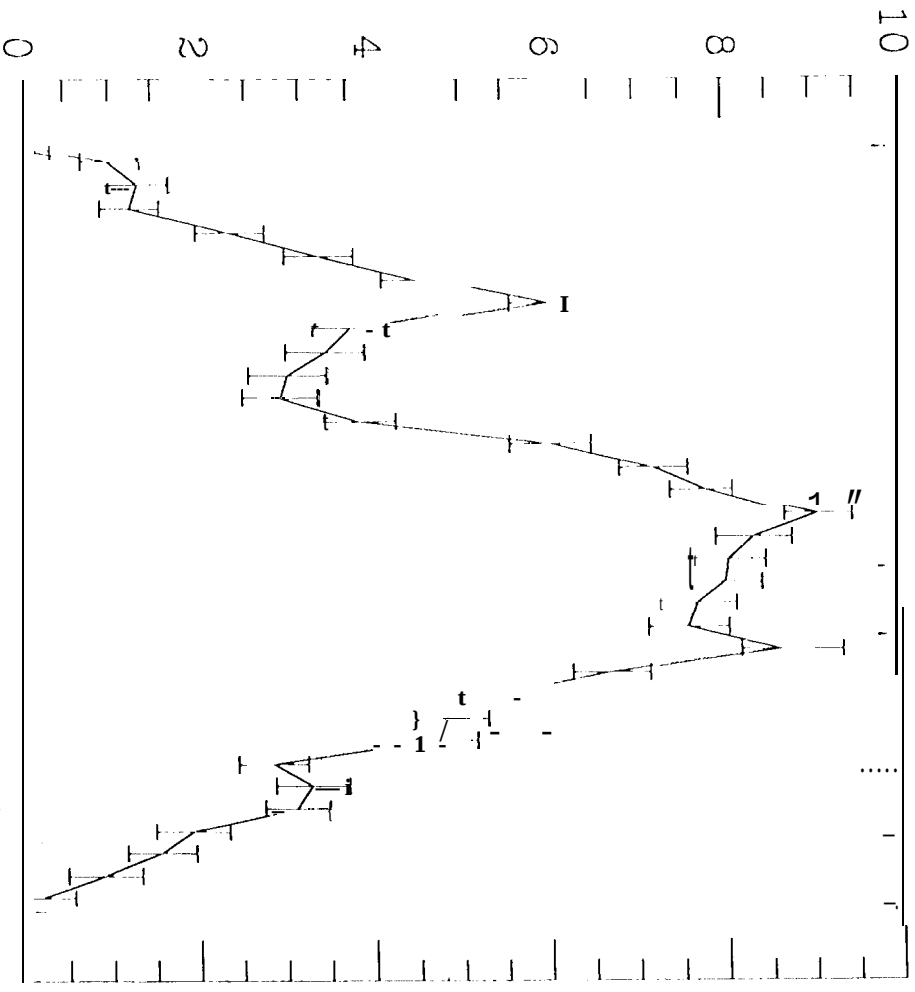

Figure 5

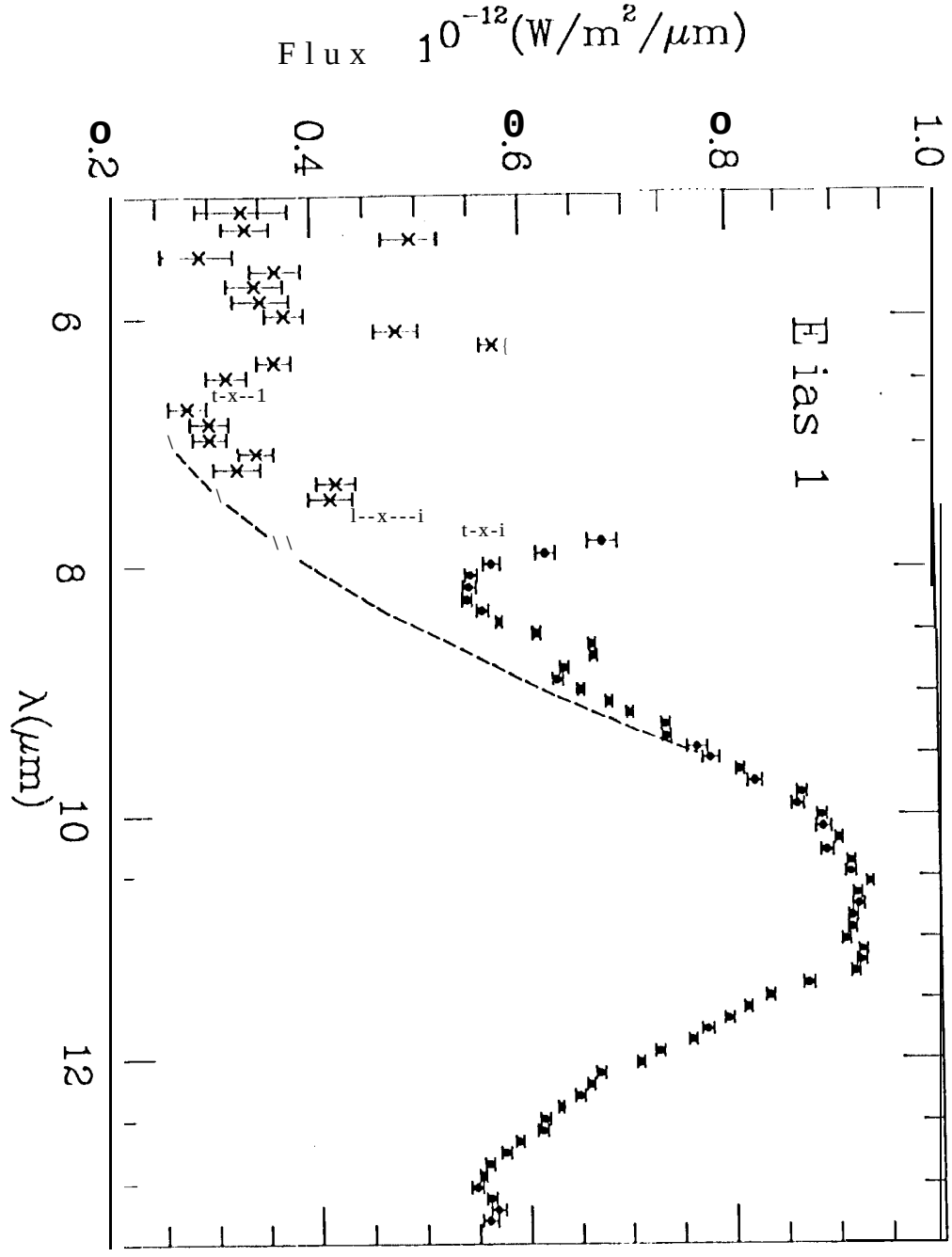
Flux $10^{-12}(W/m^2/\mu m)$
0.2
0.4
0.6
0.8
1.0
6
8
10
12
$\lambda(\mu m)$
Elias 1
t-x--1
l--x---i
t-x-i

Fig 4

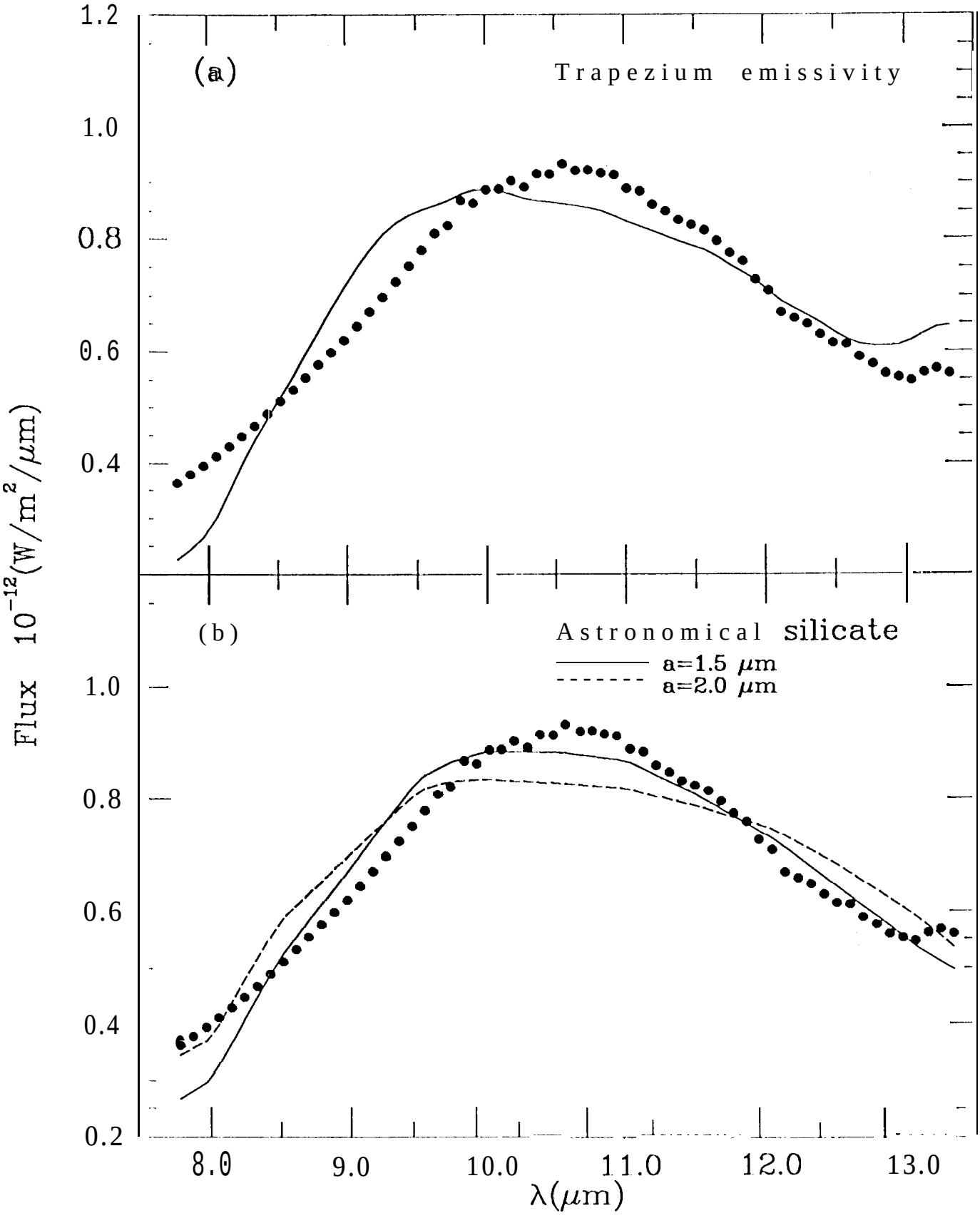
(a)
Trapezium emissivity
(b)
Astronomical silicate
a=1.5 μm
a=2.0 μm
Flux 10^{-12}(W/m^2/μm)
λ(μm)
1.2
1.0
0.8
0.6
0.4
0.2
8.0
9.0
10.0
11.0
12.0
13.0

Fig 5